International Journal Multidisciplinary
Homepage : https://journal.antispublisher.com/index.php/IJMI
Email : admin@antispublisher.com

e-ISSN : 3031-9870
IJMI, Vol. 3, No. 4, November 2026
Page 13-21

A Study of the Effect of Partial Nickel Substitution on the Structural and Magnetic Properties of $La_{0.5}Sr_{1.5}Co_{1-x}Ni_xO_4$ Composite Prepared Using an Enhanced Sol–Gel Method

Dheyab T. Noori[1], Reham Z. Hadi[2], Robak Aziz Rashid[3]
[1,2,3]Tikrit University, Iraq

DOI : https://doi.org/10.61796/ijmi.v3i4.616

Sections Info

Article history:
Submitted: June 07, 2026
Final Revised: July 26, 2026
Accepted: August 18, 2026
Published: September 10, 2026

Keywords:
X-ray diffraction
Morphological
Vibrational
Sol-gel method
Spectroscopy

ABSTRACT

Objective: *This study examines the concept of substituting one element for another in a compound and analyses the results.* ***Method:*** *The compound was synthesised and prepared using an improved sol-gel method, employing different concentrations to substitute nickel with cobalt, and investigating the effect on the material's structural, morphological, vibrational and magnetic properties.* ***Results:*** *X-ray diffraction results showed that all structural properties were retained, with a slight change in the crystal lattice and a gradual decrease in particle size as the concentration ratio changed. As for the infrared spectroscopy results, they revealed the appearance of distinctive vibrational peaks characteristic of octahedral structures, with the absence of a fingerprint region during doping at higher concentrations. As for the results of the magnetic properties analysis, it was found that the doping process results in a weakening of magnetic coupling and a shift in paramagnetic behaviour towards a softer ferromagnetic state (paramagnetic–ferromagnetic).* ***Novelty:*** *Ultimately, all the results indicated that the doping process is an effective and excellent method for controlling and enhancing the structural, magnetic and electronic properties in low-power energy-saving device applications.*

INTRODUCTION

The most important class of materials is perovskite oxides, which have recently gained significant attention in research, as they are characterised by a wide range of physical and chemical properties, including magnetic properties and electrical conductivity [1], [2] as well as high reactivity in oxidation and reduction processes. These oxides are distinguished by their layered structure, consisting of perovskite layers combined with sodium chloride layers [3]. This gives them structural flexibility, which in turn allows them to accommodate various types of crystal defects as well as ion implantation without altering or damaging the underlying structure, The family of layered cobaltate compounds of the LSR type is among the most important [4], as it exhibits complex responses and interactions between the spin, charge and orbital states of cobalt ions; this is reflected in the magnetic and electrical behaviour of cobalt, which in turn leads to partial doping in its transition elements, as well as causing significant changes in magnetic exchange interactions, thereby altering the material's overall structural and magnetic properties [5], [6], [7]. The process of cobalt doping with nickel in this system is of great importance, as the ionic radius differs between cobalt and its nickel counterpart, which in turn causes changes in the coordination angles along the superexchange pathways responsible for the magnetic ordering in these compounds. Furthermore, changes in the doping ratios of these compounds at different values

provide us with a deeper understanding of the relationship between the structural and chemical compositions and the magnetic properties of materials, which in turn opens up the possibility of designing materials whose structural and magnetic properties can be controlled, which can be utilised in a variety of applications, including electromagnets, optical applications of magnets, and spintronics. The synthesis of such compounds is currently being carried out using the wet chemical method, for the preparation of complex oxides—namely the improved sol-gel method [8], [9], [10], [11], [12], [13]. This method ensures a high degree of homogeneity at the atomic level between the various components of the materials, allowing for precise control over their chemical composition [14], [15], [16]. This enables us to obtain nanoparticles or nanogranules with very similar, yet slightly varying, sizes, particularly when we use this method to prepare mixtures or blends in a thermal furnace, which avoids many of the defects associated with the traditional method0-namely, the solid-state method—by controlling the reaction conditions and the types of curing agents. Through this method, it is possible to obtain a fine powder with a homogeneous composition whilst ensuring proportions of the likelihood of dual phases or undesirable impurities [17], [18], [19].

RESEARCH METHOD

This experimental study examined the effect of partial nickel substitution on the structural, morphological, vibrational, and magnetic properties of the layered $La_{0.7}Sr_{1.3}Co_{1-x}Ni_xO_4$ system. Two substitution levels, x = 0.5 and x = 1.0, were investigated. The samples were synthesised using an enhanced sol-gel method and thermally treated at 300 °C and 500 °C. The composition and treatment conditions were selected to permit a direct comparison of the changes associated with increasing nickel content while retaining the underlying layered oxide structure.

The prepared powders were characterised using complementary analytical techniques. X-ray diffraction (XRD) was used to identify the crystalline phase, examine peak shifts, evaluate lattice parameters, and detect possible secondary phases. Crystallite size was estimated from the diffraction data using the Debye-Scherrer relationship, $D = 0.9\lambda/(\beta \cos \theta)$, where λ is the X-ray wavelength (1.5406 Å), β is the full width at half maximum, and θ is the Bragg angle. The diffraction patterns were compared with ICDD card No. 1296-34 for phase identification.

Scanning electron microscopy (SEM) was employed to observe particle morphology, agglomeration, and dimensional changes at the two nickel-substitution levels. Fourier-transform infrared (FTIR) spectroscopy was used to identify metal-oxygen vibrational bands and other spectral features associated with the prepared structure. Magnetic measurements were evaluated from the magnetisation-field hysteresis curves, with attention to saturation magnetisation, remanent magnetisation, coercive field, and the transition between paramagnetic and weak ferromagnetic behaviour.

The results were analysed descriptively and comparatively across composition and thermal-treatment conditions. Structural changes observed by XRD were interpreted

together with the SEM morphology, FTIR vibrational response, and magnetic hysteresis behaviour. This integrated analysis was used to determine whether nickel substitution produced consistent changes across the structural, morphological, vibrational, and magnetic characteristics of the material.

RESULTS AND DISCUSSION

Results

X-ray diffraction results

Figure (1) illustrates the X-ray diffraction pattern, which indicates that these patterns retain their structural integrity without the presence of impurities. This result confirms the successful doping of nickel into cobalt sites without the formation of secondary phases, as a slight shift in the main peaks was observed when the concentration was increased from 0. 5 to 1.0 in the temperature 300 and 500 C°. In accordance with Bragg's law, this shift represents a slight contraction in the crystal lattice, caused by the substitution of nickel for cobalt without any phase transformation in the structure. As for the crystal size, it was calculated using Equation (1), the Debye–Scherrer equation [20]:

$$D = 0.9\lambda/(\beta\cos\theta) \quad (1)$$

where λ = 1.5406 Å, β = FWHM, and θ = Bragg angle.The values were approximately 3±45 at a concentration of 0.5 and 3±40 at a concentration of 1. 0. It can be observed that the size decreases as the nickel concentration increases; it can therefore be concluded that nickel doping inhibits particle growth and induces lattice strain. The peaks were matched using the ICDD global matching card No. (1296-34) and in Table 1 Crystal lattice constants and grain size

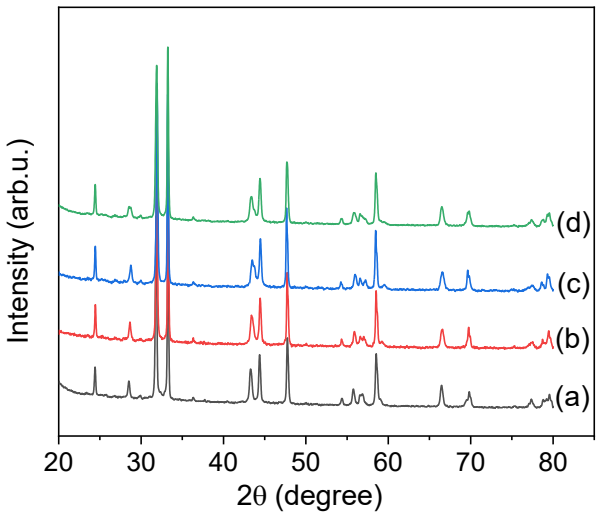

Figure 1. XRD patterns of $La_{0.7}Sr_{1.3}Co_{1-x}Ni_xO_4$ for (a)x = 0.5 in 300 C° (b) x= 0.5 in 500 C°, and (c) x = 1.0 in 300 C° , (d) x=1.0 in 500 C° .

Table 1. Crystal lattice constants and grain size

Sample	T(℃)	a (*A*°)	c (*A*°)	V (*A*°)	D_{sh}
X = 0.5	300℃	9.23	3.05	294.12	**35.71**
X = 1.0	500℃	9.23	3.05	289.24	**81.72**

Scanning electron microscope (SEM) results

The SEM images in Figure (2) show that the prepared sample, which differs in its composition and in which nickel is doped with the compound at varying ratios, has had a very significant effect on the behaviour and shape of the particles. As can be seen from the attached images with a magnification of x=0.5 in Figure (2 (a)) provide a good result, with excellent nanorods having a diameter of approximately 30–60 nanometres and a length of approximately 150–300 nanometres. This suggests that the nickel particles grow well and asymmetrically along a specific crystalline direction, which is consistent with a layered structure. whereas for a nickel doping ratio of x = 1.0 in Figure (2(b)) the change is dramatic, with the particles transforming into densely packed, irregular nanoparticles, accompanied by significant agglomeration. This differs from the first doping ratio, where no distinct structures were produced and the particle size decreased to approximately 50–90 nanometres; this may be due to surface energy. Ultimately, it can be concluded that the substitution and doping of nickel in the composite significantly alters the behaviour and morphology of the particles, transforming them from spherical to structures resembling rod-like shapes with compact agglomerates. This leads to a change in the phase growth process during fabrication and the crystallisation process.

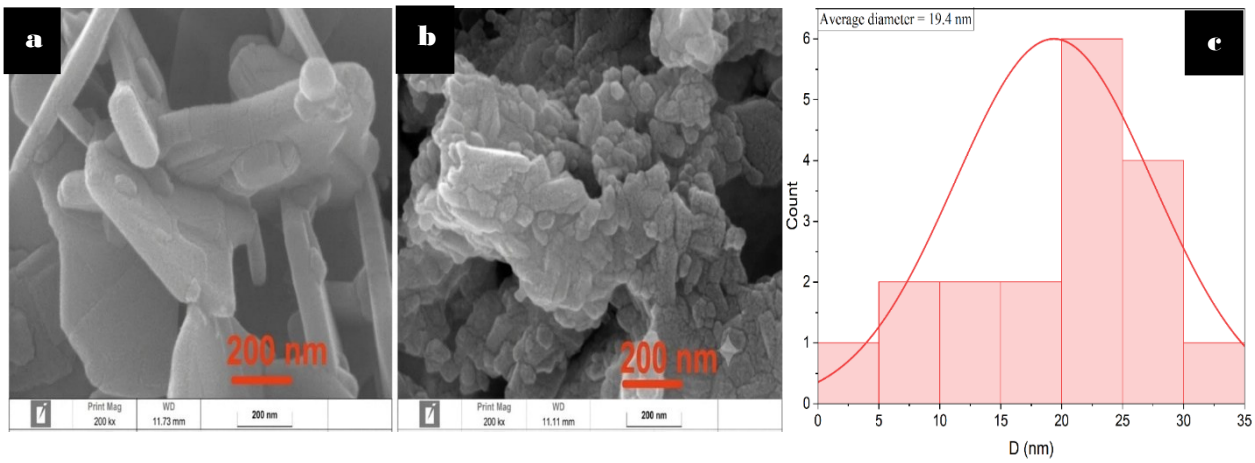

Figure 2. SEM images of $La_{0.7}Sr_{1.3}Co_{1-x}Ni_xO2$ for (a) x = 0.5, and (b) x = 1.0 , (c) Curved diameter distribution

Magnetic Force Results

Figure (3) showing the results of the magnetic measurements illustrates that, at a doping ratio of x = 0. 5, a narrowing of the magnetic hysteresis loop is observed, along

with a noticeable decrease in the remanence and saturation magnetisation. A clear and significant quasi-linear variation in the magnetic field with magnetisation is also observed, which is widely applicable; this may be due to the weak ferromagnetic component, and the results indicate that the material exhibits exhibits paramagnetic behaviour; this is due to the substitution of cobalt with nickel, which strengthens the superexchange interactions between cobalt and nickel. However, when doped at a ratio of x = 1. 0, it is observed that the magnetic lag loop becomes very narrow, with a decrease in the coercive field and a reduction in the remanence; this prevents full saturation from being reached, even at very high magnetic fields. This behaviour can be described as 'soft' for a magnetic material exhibiting a mixture of (paramagnetic–ferromagnetic) properties. It can ultimately be concluded that, as the doping ratio increases, the ferromagnetic coupling weakens compared to the original composition of the cobalt-rich compound, which may result from several factors, including slight contraction in the crystal lattice as well as a change in the balance of cobalt and nickel ions. This leads to effects on the bond angles, which in turn reduces the crystal volume and also creates crystal defects. Ultimately, it can be concluded that the magnetic results are consistent with the X-ray diffraction patterns as well as with the scanning electron microscopy results, indicating that the substitution of nickel at the concentrations studied transforms the magnetic behaviour into a mixed system that can be described as 'ferro-weak' with distinctive softness.

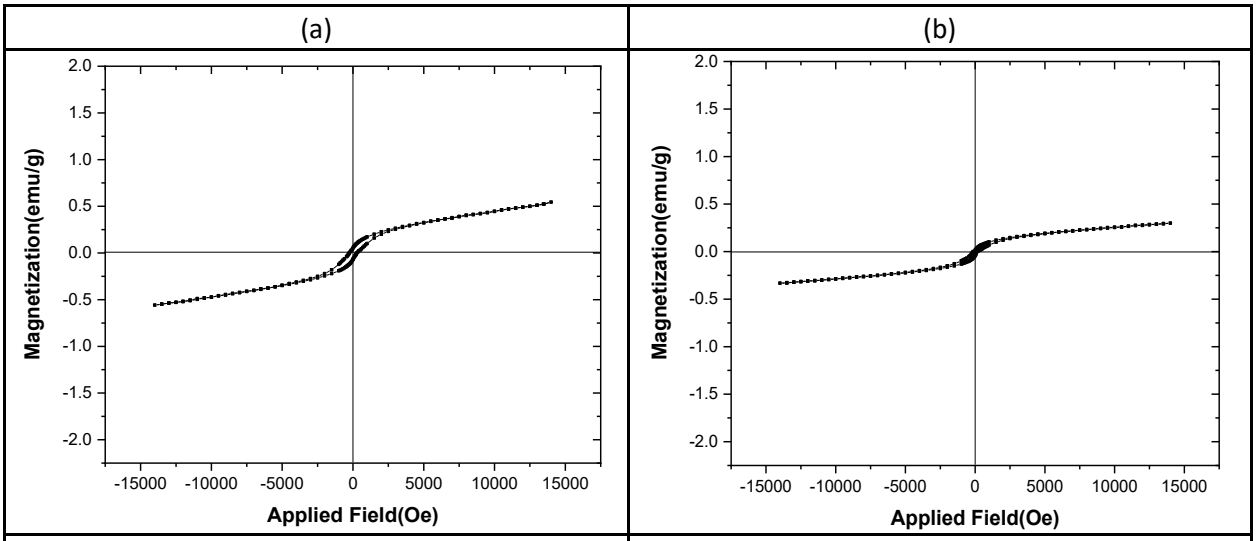

Figure 3. VSM images of $La_{0.7}Sr_{1.3}Co_{1-x}Ni_xO_4$ for, (a) x = 0.5, and (b) x = 1.0

Infrared Spectroscopy Results

Figure (4) shows that, for a substitution ratio of x = 0.5, nickel substitution results in the formation of a crystalline structure, as evidenced by the appearance of characteristic vibrational peaks in the frequency region below 700 cm^{-1}, as well as in the region with a frequency of (3000 cm^{-1}), where high-frequency peaks are observed,

indicating the presence of some surface moisture as well as a small amount of carbon residues, which may have resulted from exposure to air during the preparation process without affecting the basic structural composition. This result can be concluded to be consistent with the X-ray diffraction analysis, which shows the growth of a single-phase structure

As for Figure (5) for the ratio x = 1.0, it is observed that the sample still retains its basic structural composition, as evidenced by the appearance of Ni-O vibrational peaks in a distinct region below 800 cm^{-1}; furthermore, alongside this peak, additional peaks are observed in the frequency region below 1000 cm -1, which indicate a vibrational complex formed after substitution at the specified ratio. It can ultimately be concluded that the peaks in the higher regions are due to trace moisture, which has no effect on the basic structural composition; these results are consistent with X-ray analysis, electron microscopy and magnetic properties.

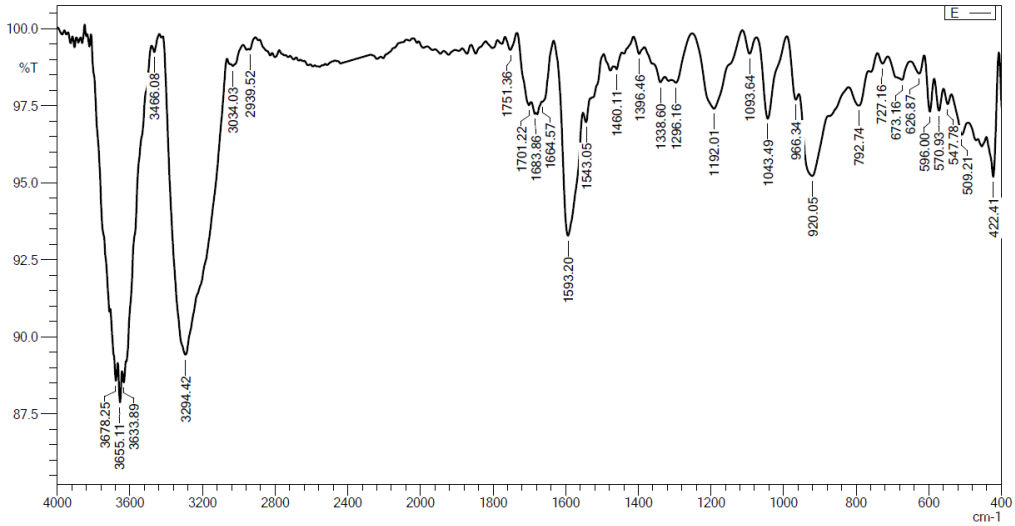

Figure 4. FTIR of $La_{0.7}Sr_{1.3}Co_{1-x}Ni_xO_4$ for, x = 0.5.

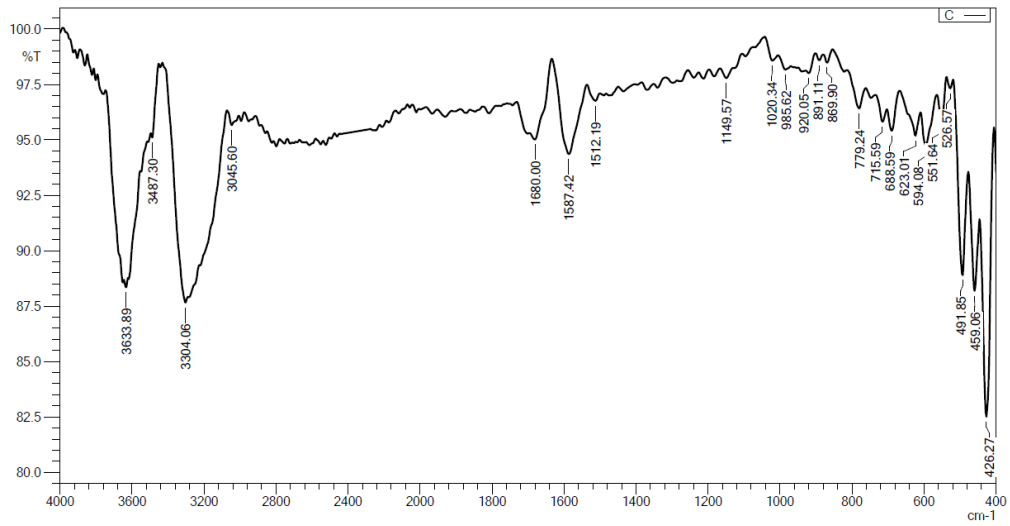

Figure 5. FTIR of $La_{0.7}Sr_{1.3}Co_{1-x}Ni_xO_4$ for, x = 1.0.

Discussion

The combined XRD, SEM, FTIR, and magnetic measurements demonstrate that increasing nickel substitution systematically modifies the structural, morphological, vibrational, and magnetic characteristics of $La_{0.7}Sr_{1.3}Co_{1-x}Ni_xO_4$ without destroying its fundamental layered structure. The slight displacement of the principal diffraction peaks and reduction in crystallite size from approximately 45 ± 3 nm at x = 0.5 to 40 ± 3 nm at x = 1.0 indicate lattice contraction and substitution-induced strain, confirming that Ni ions were incorporated into Co sites without generating detectable secondary phases. These structural changes correspond closely to the SEM observations: the well-defined nanorod morphology at x = 0.5 develops into smaller, densely agglomerated, and irregular nanoparticles at x = 1.0, suggesting that higher nickel content restricts anisotropic particle growth and alters the crystallisation mechanism. The FTIR bands below 700–800 cm^{-1} further support the preservation of metal–oxygen coordination within the oxide framework, whereas the additional bands below 1000 cm^{-1} at x = 1.0 indicate changes in the local vibrational environment following substitution. The weak high-frequency bands are most reasonably associated with adsorbed moisture or residual carbon species and therefore do not contradict the single-phase structure observed by XRD. Magnetically, the increasingly narrow hysteresis loop, reduced remanent magnetisation, lower coercivity, and incomplete saturation indicate a transition toward mixed paramagnetic–weak-ferromagnetic behaviour with soft-magnetic characteristics. This response may be attributed to lattice contraction, structural defects, altered Co–O–Ni bond geometry, and disruption of long-range exchange interactions as the nickel concentration increases. Overall, the agreement among the four characterisation techniques shows that nickel substitution provides an effective route for tuning the structure and magnetic softness of the material, supporting its potential use in low-power spintronic, magnetic, electronic, and optoelectronic devices; nevertheless, measurements of electrical transport, optical response, thermal stability, and device-level performance are still required to confirm these prospective applications.

CONCLUSION

Fundamental Finding: The analyses consistently demonstrated that nickel substitution caused crystal lattice contraction, infrared spectral shifts, a gradual reduction in grain size, and weakened long-range magnetic coupling. **Implication:** The substitution of nickel with cobalt effectively controls the material's magnetic and structural properties, making it a promising candidate for multifunctional applications in spintronic, electronic, magnetic, and optoelectronic fields. **Limitation:** The study was limited to the investigated substitution levels and characterization techniques, without evaluating the material's performance under actual device operating conditions. **Future Research:** Further studies should investigate broader substitution ranges, additional electronic and optical properties, long-term material stability, and practical device integration to confirm its suitability for multifunctional applications.

REFERENCES

[1] C. Goswami, B. Chutia, and P. Bharali, "Metal and metal oxide-based nanomaterials for electrochemical applications," in *Nanomaterials for Sustainable Energy*, 2019. doi: 10.1007/978-3-030-04474-9_12.

[2] Y. Badour, "Unlocking the potential of photochromic tungsten oxide (WO_{3-x}) materials: Synthesis, characterization, and shaping of hybrid organic–inorganic WO_3-doped systems (0D, 1D, and 2D) for optical applications," HAL, 2023.

[3] M. U. Nisa, N. Nadeem, M. Yaseen, J. Iqbal, M. Zahid, Q. Abbas, G. Mustafa, and I. Shahid, "Applications of graphene-based tungsten oxide nanocomposites: A review," *J. Nanostruct. Chem.*, vol. 13, pp. 167–196, 2022. doi: 10.1007/s40097-021-0046.

[4] A. Mashhadian, R. Jian, S. Tian, S. Wu, and G. Xiong, "An overview of electrochemical sensors based on transition metal carbides and oxides: Synthesis and applications," *Micromachines*, vol. 15, 2024. doi: 10.3390/mi15010042.

[5] A. B. Sengul and E. Asmatulu, "Toxicity of metal and metal oxide nanoparticles: A review," *Environ. Chem. Lett.*, vol. 18, pp. 1659–1683, 2020. doi: 10.1007/s10311-020-01033-6.

[6] S. Murthy, P. Effiong, and C. C. Fei, "Metal oxide nanoparticles in biomedical applications," in *Metal Oxide Nanoparticles in Biomedical Applications*. Amsterdam, The Netherlands: Elsevier, 2020. doi: 10.1016/B978-0-12-817505-7.00011-7.

[7] M. Modak, S. Rane, and S. Jagtap, "WO_3: A review of synthesis techniques, nanocomposite materials and their morphological effects for gas sensing application," *Bull. Mater. Sci.*, vol. 46, 2023. doi: 10.1007/s12034-022-02864-5.

[8] J. Gupta, H. Shaik, and K. N. Kumar, "A review on the prominence of porosity in tungsten oxide thin films for electrochromism," *Ionics*, vol. 27, pp. 2307–2334, 2021. doi: 10.1007/s11581-021-04035-8.

[9] M. Zhang, C. Yang, Z. Zhang, W. Tian, B. Hui, J. Zhang, and K. Zhang, "Tungsten oxide polymorphs and their multifunctional applications," *Adv. Colloid Interface Sci.*, vol. 300, Art. no. 102596, 2022. doi: 10.1016/j.cis.2021.102596.

[10] S. Cong, F. Geng, and Z. Zhao, "Tungsten oxide materials for optoelectronic applications," *Adv. Mater.*, vol. 28, pp. 10518–10528, 2016. doi: 10.1002/adma.201601109.

[11] A. H. Y. Hendi, M. F. Al-Kuhaili, S. M. A. Durrani, M. M. Faiz, A. Ul-Hamid, A. Qurashi, and I. Khan, "Modulation of the band gap of tungsten oxide thin films through mixing with cadmium telluride towards photovoltaic applications," *Mater. Res. Bull.*, vol. 87, pp. 148–154, 2017. doi: 10.1016/j.materresbull.2016.11.032.

[12] D. J. Trainer, J. Nieminen, F. Bobba, B. Wang, X. Xi, A. Bansil, and M. Iavarone, "Visualization of defect-induced in-gap states in monolayer MoS_2," *npj 2D Mater. Appl.*, vol. 6, pp. 1–7, 2022. doi: 10.1038/s41699-022-00286-9.

[13] Y. Wang, P. Yang, L. Zheng, X. Shi, and H. Zheng, "Carbon nanomaterials with sp^2 or/and sp hybridization in energy conversion and storage applications: A review," *Energy Storage Mater.*, vol. 26, pp. 349–370, 2020. doi: 10.1016/j.ensm.2019.11.006.

[14] F. P. Netzer, "Small and beautiful—The novel structures and phases of nano-oxides," *Surf. Sci.*, vol. 604, pp. 485–489, 2010.

[15] F. P. Netzer, F. Allegretti, and S. Surnev, "Low-dimensional oxide nanostructures on metals: Hybrid systems with novel properties," *J. Vac. Sci. Technol. B*, vol. 28, no. 1, pp. 1–16, 2010.

[16] N. Nilius, "Properties of oxide thin films and their adsorption behavior studied by scanning tunneling microscopy and conductance spectroscopy," *Surf. Sci. Rep.*, vol. 64, pp. 595–659, 2009.

[17] H.-J. Freund and G. Pacchioni, "Oxide ultra-thin films on metals: New materials for the design of supported metal catalysts," *Chem. Soc. Rev.*, vol. 37, pp. 2224–2242, 2008.
[18] L. Giordano and G. Pacchioni, "Oxide films at the nanoscale: New structures, new functions, and new materials," *Acc. Chem. Res.*, vol. 44, pp. 1244–1252, 2011.
[19] C. Xu, M. Zhu, Q. Wang, J. Cui, Y. Huang, X. Huang, J. Huang, J. Gai, G. Li, P. Qiao, *et al.*, "TROP2-directed nanobody-drug conjugate elicited potent antitumor effect in pancreatic cancer," *J. Nanobiotechnol.*, vol. 21, Art. no. 410, 2023.
[20] X. Pi, D. Yan, Y. Xu, M. Pan, Z. Wang, M. Chang, and Z. Qi, "TLRs signaling pathway regulation, antibacterial and apoptotic activity of largemouth bass ECSIT during *Edwardsiella piscicida* infection," *Aquaculture*, vol. 595, Art. no. 741615, 2025.

***Dheyab T. Noori (Corresponding Author)**
Tikrit University, Iraq
Email: theyab.thair.tuz@tu.edu.iq

Reham Z. Hadi
Tikrit University, Iraq
Email: reham.z.hadi@tu.edu.iq

Robak Aziz Rashid
Tikrit University, Iraq
Email: Rupak.A.Rasheed@tu.edu.iq